

Received May 22, 2019, accepted June 11, 2019, date of publication June 14, 2019, date of current version July 3, 2019.

Digital Object Identifier 10.1109/ACCESS.2019.2922972

VLF Current Distribution and Input Impedance of an Arbitrarily Oriented Linear Antenna in a Cold Plasma

TONG HE^{ID}, (Student Member, IEEE), HUI RAN ZENG^{ID}, (Student Member, IEEE), AND KAI LI^{ID}

College of Information Science and Electronic Engineering, Zhejiang University, Hangzhou 310027, China

Corresponding author: Kai Li (kaili@zju.edu.cn)

This work was supported by the National Science Foundation of China under Grant 61571389 and Grant 61271086.

ABSTRACT In this paper, we proposed a semianalytical method for calculating the current distribution and input impedance of a very low frequency (VLF: 3–30 kHz) linear antenna of arbitrary orientation in a homogeneous anisotropic cold plasma. By considering the effect of the geomagnetic inclination angle, the kernel function, in this case, has a more complicated form and requires extra analytical techniques to deal with. The computations show that the amplitude coefficients for the ordinary wave are evidently greater than those for the extraordinary wave. We also found that the shape of the current distribution is not sensitive to the orientation of the antenna, but the total current moment on the antenna will be decreased when the inclination angle becomes larger. Moreover, due to the higher attenuation rates for both the ordinary and extraordinary waves at a propagation direction perpendicular to the magnetic field, the overall trend for the input impedance of the antenna is increasing with the geomagnetic inclination angle. It is then concluded that the optimal posture for a VLF space-borne linear antenna should be as parallel as possible to the direction of the geomagnetic field in order to achieve maximum antenna efficiency.

INDEX TERMS Anisotropic plasma, arbitrary oriented linear antenna, input impedance, VLF electromagnetic wave.

I. INTRODUCTION

As important and useful devices in information transmission systems, linear antennas have been extensively studied during the past few decades. It is known that the very low frequency (VLF: 3–30 kHz) is the feasible frequency band for over-water/underwater communications and navigation. However, most of the existing VLF communication systems were built on huge ground-based transmitting stations, which not only required large investments but also were difficult to repair in short time once damaged. Fortunately, with the progress of space technology and the decrease on satellite launching costs, it is now possible to develop a VLF space-borne transmitting system. One of the feasible ideas was to tether the antenna to a near-earth satellite which usually operated at a low earth orbit of 300–400 km. For one thing, the ionospheric plasma (F_2 layer) surrounding a space-borne antenna has a large refractive index of 50–150 in the VLF range [1], thus the electrical length of the antenna can be greatly increased

The associate editor coordinating the review of this manuscript and approving it for publication was Luca Chiaraviglio.

without increasing the geometric size. On the other hand, the electron density at this height is relatively stable [2], so it is reasonable to take the ambient environment of the antenna as a homogeneous plasma when the propagation distance is not too far. Since the 1980s, several countries especially including the U.S. and Russia had started the investigations on VLF space-borne transmitting and propagation experiments [3]–[7]. In the joint project launched by NASA and the Italian Space Agency (ASI) in 1992 [8], the tethered satellite system (TSS) was connected to a space shuttle by a 20 kilometers long conducting tether, where the tether was regarded as a linear antenna for transmitting VLF signals. It is worth mentioning that the successful experiments implemented by the U.S. and Russia had validated that VLF waves transmitted by a space-borne antenna could effectively propagate in the ionosphere and finally reach the sea surface with detectable amplitudes [4], [6].

Relevant studies on the theory of linear antennas in plasmas were also carried out by many researchers. In 1964, the first analytical expressions for the impedance of a short electric dipole antenna in a cold magnetoplasma were examined

by Balmain [9]. In early 1970s, Wang and Bell [10]–[12] derived the formulas for the radiation resistance and radiation pattern of an arbitrarily oriented electric dipole antenna in a cold magnetoplasma. The impedance of a dipole antenna in a near-isotropic ionosphere was then investigated by Vernet *et al.* [13] and Meyer and Vernet [14] both theoretically and experimentally in 1975. In 2001, the radiation impedance of a short dipole antenna in a cold collisional plasma was calculated by Nikitin and Swenson [15] using a quasi-static method. Subsequently, Bell *et al.* [16] performed detailed studies on the closed-form solutions for the current distribution on an electric dipole antenna operating in the plasmasphere. In 2008, the current distribution and terminal impedance of a VLF electric dipole antenna in a cold magnetoplasma were obtained by Chevalier *et al.* [17] through finite-difference-frequency-domain (FDTD) simulations. In 2015, Chugunov *et al.* [18] proposed a method for calculating the charge distribution and impedance of a short cylindrical antenna at different orientations relative to the anisotropy axis of the medium. In a more recent paper by He *et al.* [19], the analytical formulas for the current distribution and input impedance of a thin linear antenna oriented along the magnetic field in an anisotropic plasma were derived.

It is known that the efficiency of a linear antenna is largely dependent on the total current moment on the antenna as well as the input impedance. However, due to the complex anisotropic characteristics of the ionosphere at the VLF range, calculating the current distribution and input impedance of a VLF space-borne antenna has never been an easy task. When considering the ionospheric anisotropy, VLF waves transmitted by a space-borne antenna will be divided into two modes, i.e., the ordinary wave (O-wave) and the extraordinary wave (E-wave). At heights of a near-earth satellite, the O-wave is an evanescent wave, thereby its influences were usually neglected when discussing the far-field. While the E-wave is the propagable mode with a small attenuation rate as long as the propagation direction is within the critical angle [20]. Considering the current distribution and input impedance of an antenna are mainly determined by its near-field and VLF wavelengths will be greatly shortened in the ionosphere, the ambient medium of a VLF space-borne antenna can be regarded as a homogeneous anisotropic plasma and both the contributions of the O-wave and E-wave should be taken into account. It is noted that the angle between a real space-borne antenna and the geomagnetic field may not be fixed, but will change with the satellite moving along the orbit [21]. Also, the importance of antenna orientation relative to the magnetic field in space plasmas had been emphasized in a review by James [22]. Unfortunately, most of the existing works only tackled the radiation resistance of the antenna with an assumed current distribution, but few of them had dedicated to computing the current distribution and input impedance when the antenna is at arbitrary orientations to the background magnetic field. Therefore, in order to further analyze the effect of the geomagnetic inclination angle, it is

necessary to conduct a more comprehensive study on this problem and seek effective methods for calculation of the current distribution and input impedance of an arbitrarily oriented space-borne linear antenna.

In this paper, by extending the analysis to a more general case, we will attempt to propose a possible semi-analytical method to solve the current distribution and input impedance of a VLF space-borne linear antenna at arbitrary orientations to the geomagnetic field. This method is particularly applicable to the cases when the drive voltage applied on the antenna is relatively small compared to the background plasma potential. As such, the ionospheric environment surrounding the antenna is assumed to be a cold plasma region with all the nonlinear sheath effects and wave-particle interactions neglected. The kernel function in this case, which has a more complicated form due to considering the antenna orientation, is also derived. The results of this paper draw some conclusions that are in good agreement with those in [12], [17] and may provide heuristic suggestions to the overall design of a practical VLF space-borne transmitting system.

II. FORMULATIONS OF THE PROBLEM

A. ELECTRIC FIELD EXCITED BY AN ARBITRARILY ORIENTED ELECTRIC DIPOLE

For a linear antenna of arbitrary direction, we let the static magnetic field always be parallel to the \hat{z} axis, while adjust the orientation of the antenna in the meantime. By using a cold plasma treatment, the relative dielectric tensor for the ambient ionosphere derived from a fluid model is expressed as

$$\hat{\epsilon} = \begin{bmatrix} \epsilon_1 & -i\epsilon_2 & 0 \\ i\epsilon_2 & \epsilon_1 & 0 \\ 0 & 0 & \epsilon_3 \end{bmatrix} \quad (1)$$

where

$$\epsilon_1 = 1 - \frac{XU}{(U^2 - Y^2)} \quad (2)$$

$$\epsilon_2 = \frac{XY}{(U^2 - Y^2)} \quad (3)$$

$$\epsilon_3 = 1 - \frac{X}{U} \quad (4)$$

$$U = 1 + i\frac{\nu}{\omega}, \quad X = \frac{\omega_0^2}{\omega^2}, \quad Y = \frac{\omega_H}{\omega} \quad (5)$$

$$\omega_0^2 = \frac{Ne^2}{\epsilon_0 m_e}, \quad \omega_H = \left| \frac{eB_0}{m_e} \right| \quad (6)$$

In above formulas, ω_0 , ω_H , and ω are the plasma frequency, gyro frequency, and operating angular frequency, respectively. The magnitude of the geomagnetic field is denoted by B_0 , while m_e , e are the mass and charge quantity of an electron, respectively. The electron density and collision frequency of the ionosphere are denoted by N and ν , respectively. ϵ_0 , μ_0 , and $k_0 = \omega\sqrt{\mu_0\epsilon_0}$ are the permittivity, permeability, and wave number in free space, respectively. In the

whole text, the time harmonic factor $\exp(-i\omega t)$ is assumed and suppressed.

With a 3-D Fourier transform employed, the electric field excited by an electric dipole with current moment $I \cdot dl = 1$ in an infinite homogeneous anisotropic ionosphere could be expressed in a triple integral form [23]. By converting the formula from spherical coordinates to a cylindrical coordinate system, we have

$$E(\rho, \varphi, z) = \frac{-i\omega\mu_0}{(2\pi)^3} \int_{-\infty}^{\infty} dk_z \int_0^{2\pi} d\varphi_k \int_0^{\infty} \frac{F(k_z, \lambda, \varphi_k)}{B(k_z, \lambda)} \times \exp\{-i[k_z z + \lambda\rho \cos(\varphi - \varphi_k)]\} \lambda d\lambda \quad (7)$$

where

$$B(k_z, \lambda) = k_0^6 \left[\left(\frac{k_z}{k_0}\right)^4 \varepsilon_3 + \left(\frac{\lambda}{k_0}\right)^2 (\varepsilon_2^2 - \varepsilon_1^2 - \varepsilon_1 \varepsilon_3) + \left(\frac{k_z}{k_0}\right)^2 \left(\frac{\lambda}{k_0}\right)^2 (\varepsilon_1 + \varepsilon_3) - 2 \left(\frac{k_z}{k_0}\right)^2 \varepsilon_1 \varepsilon_3 + \varepsilon_3 (\varepsilon_1^2 - \varepsilon_2^2) + \left(\frac{\lambda}{k_0}\right)^4 \varepsilon_1 \right] \quad (8)$$

Here the dipole is assumed to be located at the origin, and $F(k_z, \lambda, \varphi_k)$ is a function related to the direction of the dipole. When the dipole is oriented along the \hat{z} axis (parallel to the magnetic field), the components of F^z are

$$F_x^z = k_z \lambda (k_z^2 + \lambda^2 - k_0^2 \varepsilon_1) \cos \varphi_k - ik_z \lambda k_0^2 \varepsilon_2 \sin \varphi_k \quad (9)$$

$$F_y^z = k_z \lambda (k_z^2 + \lambda^2 - k_0^2 \varepsilon_1) \sin \varphi_k + ik_z \lambda k_0^2 \varepsilon_2 \cos \varphi_k \quad (10)$$

$$F_z^z = (k_z^2 + \lambda^2) k_z^2 - k_0^2 \varepsilon_1 (2k_z^2 + \lambda^2) + k_0^4 (\varepsilon_1^2 - \varepsilon_2^2) \quad (11)$$

If the dipole is oriented along the \hat{x} axis (perpendicular to the magnetic field), the components of F^x are given by

$$F_x^x = k_0^2 (k_0^2 \varepsilon_1 \varepsilon_3 - \varepsilon_1 \lambda^2 - \varepsilon_3 k_z^2) + \lambda^2 (k_z^2 + \lambda^2 - k_0^2 \varepsilon_3) \cos^2 \varphi_k \quad (12)$$

$$F_y^x = -ik_0^2 \varepsilon_2 (k_0^2 \varepsilon_3 + \lambda^2) - \lambda^2 (k_z^2 + \lambda^2 - k_0^2 \varepsilon_3) \sin \varphi_k \cos \varphi_k \quad (13)$$

$$F_z^x = k_z \lambda \left(k_z^2 + \lambda^2 - k_0^2 \varepsilon_1 \right) \cos \varphi_k + ik_z \lambda k_0^2 \varepsilon_2 \sin \varphi_k \quad (14)$$

For the purpose of simplification, we put the dipole in the \hat{x} - \hat{z} plane by rotating the coordinate axes. Thereby an arbitrarily oriented electric dipole can be taken as a superposition of the above two cases. If we define the angle between the dipole and the \hat{z} axis as θ_b , then the function F^{θ_b} for an electric dipole at an angle of θ_b relative to the magnetic field should satisfy the following relations

$$\begin{bmatrix} F_x^{\theta_b} \\ F_y^{\theta_b} \\ F_z^{\theta_b} \end{bmatrix} = \begin{bmatrix} F_x^z \\ F_y^z \\ F_z^z \end{bmatrix} \cos \theta_b + \begin{bmatrix} F_x^x \\ F_y^x \\ F_z^x \end{bmatrix} \sin \theta_b \quad (15)$$

In this study, the tangential electric field along the direction of the antenna is of our primary interest. Considering the arbitrarily oriented electric dipole is in the \hat{x} - \hat{z} plane, the corresponding component of F^{θ_b} for the tangential electric field

of a dipole at θ_b could be written in the following form

$$F_{tan}^{\theta_b} = F_z^{\theta_b} \cos \theta_b + F_x^{\theta_b} \sin \theta_b = F_z^z \cos^2 \theta_b + F_x^x \sin^2 \theta_b + (F_z^x + F_x^z) \sin \theta_b \cos \theta_b \quad (16)$$

It is seen that for $\theta_b = 0^\circ$, $F_{tan}^{\theta_b}$ reduces to F_z^z , and if $\theta_b = 90^\circ$, the above equation reduces to F_x^x . Besides, the tangential component of the electric field in this case is expressed by

$$E_{tan}^{\theta_b}(\rho, \varphi, z) = \frac{-i\omega\mu_0}{(2\pi)^3} \int_{-\infty}^{\infty} dk_z \int_0^{2\pi} \int_0^{\infty} \frac{F_{tan}^{\theta_b}(k_z, \lambda, \varphi_k)}{B(k_z, \lambda)} \times \exp\{-i[k_z z + \lambda\rho \cos(\varphi - \varphi_k)]\} \lambda d\lambda d\varphi_k \quad (17)$$

Now we introduce the integral form for the Bessel function. It is [24]

$$J_n(\lambda\rho) = \frac{i^{-n}}{2\pi} \int_0^{2\pi} \exp(i\lambda\rho \cos \theta) \exp(in\theta) d\theta \quad (18)$$

By letting $\theta = \varphi - \varphi_k$, it follows that

$$\int_0^{2\pi} \exp[-i\lambda\rho \cos(\varphi - \varphi_k)] d\varphi_k = 2\pi J_0(\lambda\rho) \quad (19)$$

$$\int_0^{2\pi} \exp[-i\lambda\rho \cos(\varphi - \varphi_k)] \cos \varphi_k d\varphi_k = -2\pi i \cos \varphi J_1(\lambda\rho) \quad (20)$$

$$\int_0^{2\pi} \exp[-i\lambda\rho \cos(\varphi - \varphi_k)] \cos^2 \varphi_k d\varphi_k = \pi [J_0(\lambda\rho) - J_2(\lambda\rho) \cos 2\varphi] \quad (21)$$

Considering the relation between J_0 , J_1 , and J_2 is

$$J_0(\lambda\rho) + J_2(\lambda\rho) = \frac{2}{\lambda\rho} J_1(\lambda\rho) \quad (22)$$

by substituting (9)-(16) into (17) and using (19)-(22), the integral with respect to φ_k can be expressed with J_0 and J_1 and the original triple integral in (17) is reduced to a double integral. After rearrangements, Eq. (17) becomes

$$E_{tan}^{\theta_b}(\rho, \varphi, z) = \frac{-i\omega\mu_0}{(2\pi)^2} \int_{-\infty}^{\infty} \exp(-ik_z z) dk_z \times \int_0^{\infty} \left[\frac{\cos^2 \theta_b S_1(k_z, \lambda) + \sin^2 \theta_b S_2(k_z, \lambda, \varphi)}{B(k_z, \lambda)} J_0(\lambda\rho) + \frac{\sin^2 \theta_b S_3(k_z, \lambda, \varphi) + \sin \theta_b \cos \theta_b S_4(k_z, \lambda, \varphi)}{B(k_z, \lambda)} J_1(\lambda\rho) \right] \lambda d\lambda \quad (23)$$

where

$$S_1(k_z, \lambda) = (k_z^2 + \lambda^2) k_z^2 - k_0^2 \varepsilon_1 (2k_z^2 + \lambda^2) + k_0^4 (\varepsilon_1^2 - \varepsilon_2^2) \quad (24)$$

$$S_2(k_z, \lambda, \varphi) = k_0^2 \left(k_0^2 \varepsilon_1 \varepsilon_3 - \varepsilon_1 \lambda^2 - \varepsilon_3 k_z^2 \right) + \left(\frac{\cos 2\varphi + 1}{2} \right) \lambda^2 \left(k_z^2 + \lambda^2 - k_0^2 \varepsilon_3 \right) \quad (25)$$

$$S_3(k_z, \lambda, \varphi) = -\lambda \left(k_z^2 + \lambda^2 - k_0^2 \varepsilon_3 \right) \left(\frac{\cos 2\varphi}{\rho} \right) \quad (26)$$

$$S_4(k_z, \lambda, \varphi) = -2ik_z \lambda \left(k_z^2 + \lambda^2 - k_0^2 \varepsilon_1 \right) \cos \varphi \quad (27)$$

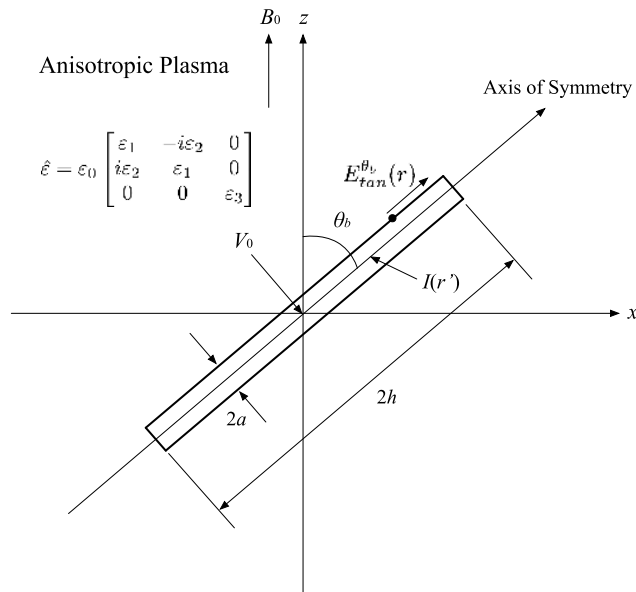


FIGURE 1. Geometry and notations of an arbitrarily oriented linear antenna in an infinite homogeneous anisotropic plasma.

Eq. (23) is the final formula for the tangential electric field component that is needed in the following analysis.

B. CURRENT DISTRIBUTION ON A VLF SPACE-BORNE LINEAR ANTENNA

The physical model of the present problem is illustrated in Fig. 1. The center-driven linear antenna has symmetric vertices with the feeding point located at the origin. The radius and half length of the antenna are denoted by a and h , with the condition $a \ll h$ satisfied. Since the ambient environment is homogeneous and the antenna is very thin, it is reasonable to assume that the current will aggregate on the central axis of the antenna. If we let $I(r')$ denote the current distribution on the antenna, while let r denote an observation point located at the surface of the antenna and in the $\hat{x}\text{-}\hat{z}$ plane simultaneously, then the tangential electric field at the outer surface of the antenna can be expressed as follows

$$E_{tan}^{\theta_b}(r) = \frac{-i\omega\mu_0}{(2\pi)^2} \int_{-h}^h G(\rho^*, \varphi^*, z^*) I(r') dr' \quad (28)$$

where the kernel function $G(\rho^*, \varphi^*, z^*)$ is given by

$$\begin{aligned} G(\rho^*, \varphi^*, z^*) &= \int_{-\infty}^{\infty} \exp(-ik_z z^*) dk_z \\ &\times \int_0^{\infty} \left[\frac{\cos^2 \theta_b S_1(k_z, \lambda) + \sin^2 \theta_b S_2(k_z, \lambda, \varphi^*)}{B(k_z, \lambda)} J_0(\lambda \rho^*) \right. \\ &\left. + \frac{\sin^2 \theta_b S_3(k_z, \lambda, \varphi^*) + \sin \theta_b \cos \theta_b S_4(k_z, \lambda, \varphi^*)}{B(k_z, \lambda)} J_1(\lambda \rho^*) \right] \lambda d\lambda \end{aligned} \quad (29)$$

It is noted that (ρ^*, φ^*, z^*) represents the relative coordinate between r and r' . We have

$$\rho^* = |(r - r') \sin \theta_b - a \cos \theta_b| \quad (30)$$

$$z^* = (r - r') \cos \theta_b + a \sin \theta_b \quad (31)$$

$$\varphi^* = \begin{cases} 0, & \text{if } (r - r') \sin \theta_b - a \cos \theta_b \geq 0 \\ \pi, & \text{if } (r - r') \sin \theta_b - a \cos \theta_b < 0 \end{cases} \quad (32)$$

Since antennas can be regarded as good conductors, according to the boundary condition, the tangential electric field at the surface of the antenna should always equal to zero. In addition, the tangential component of the electric field at the feeding point should approximately equal to the drive voltage if the feeding gap is adequately small. Considering all of the above, the boundary condition satisfied by the antenna is

$$E_{tan}^{\theta_b}(r) = -V_0 \delta(r), \quad -h < r < h \quad (33)$$

where V_0 denotes the drive voltage and $\delta(r)$ is the Dirac delta function.

According to the theory proposed by King *et al.* [25], the current distribution of a center-driven linear antenna in a homogeneous isotropic medium consists of three sinusoid current terms with an exponential decaying factor. By using a similar method with King and taking into account the effects of both the O-wave and E-wave in an anisotropic ionosphere, the current distribution on a VLF space-borne linear antenna can be derived as

$$\begin{aligned} I(r') &= \left\{ A_o \sin[\beta_o(h - |r'|)] + B_o [\cos(\beta_o r') - \cos(\beta_o h)] \right. \\ &\left. + C_o \left[\cos\left(\frac{\beta_o r'}{2}\right) - \cos\left(\frac{\beta_o h}{2}\right) \right] \right\} e^{-\alpha_o |r'|} \\ &+ \left\{ A_e \sin[\beta_e(h - |r'|)] + B_e [\cos(\beta_e r') - \cos(\beta_e h)] \right. \\ &\left. + C_e \left[\cos\left(\frac{\beta_e r'}{2}\right) - \cos\left(\frac{\beta_e h}{2}\right) \right] \right\} e^{-\alpha_e |r'|} \end{aligned} \quad (34)$$

where $A_o, B_o, C_o, A_e, B_e,$ and C_e are complex amplitude coefficients for the O-wave and E-wave, respectively, which are yet to be determined. Besides, $\beta_o, \alpha_o, \beta_e,$ and α_e are the phase constants and attenuation rates for the O-wave and E-wave, respectively. We write

$$k_o = \beta_o + i\alpha_o, \quad k_e = \beta_e + i\alpha_e \quad (35)$$

and the formulas for the wave numbers of the O-wave (k_o) and the E-wave (k_e) as a function of θ_b are given by

$$\begin{aligned} k_{o,e}^2 &= \frac{k_0^2}{2(\epsilon_1 \sin^2 \theta_b + \epsilon_3 \cos^2 \theta_b)} \left[\epsilon_1 \epsilon_3 (1 + \cos^2 \theta_b) + (\epsilon_3^2 - \epsilon_2^2) \sin^2 \theta_b \right. \\ &\left. \pm \sqrt{(\epsilon_1^2 - \epsilon_2^2 - \epsilon_1 \epsilon_3)^2 \sin^4 \theta_b + 4\epsilon_2^2 \epsilon_3^2 \cos^2 \theta_b} \right] \end{aligned} \quad (36)$$

Now we will solve the six indeterminate coefficients via the boundary condition. Let

$$I_1(r') = \exp(-\alpha_o |r'|) \sin[\beta_o(h - |r'|)] \quad (37)$$

$$I_2(r') = \exp(-\alpha_o|r'|) [\cos(\beta_o r') - \cos(\beta_o h)] \quad (38)$$

$$I_3(r') = \exp(-\alpha_o|r'|) \left[\cos\left(\frac{\beta_o r'}{2}\right) - \cos\left(\frac{\beta_o h}{2}\right) \right] \quad (39)$$

$$I_4(r') = \exp(-\alpha_e|r'|) \sin[\beta_e(h - |r'|)] \quad (40)$$

$$I_5(r') = \exp(-\alpha_e|r'|) [\cos(\beta_e r') - \cos(\beta_e h)] \quad (41)$$

$$I_6(r') = \exp(-\alpha_e|r'|) \left[\cos\left(\frac{\beta_e r'}{2}\right) - \cos\left(\frac{\beta_e h}{2}\right) \right] \quad (42)$$

and

$$V_j(r) = \int_{-h}^h G(\rho^*, \varphi^*, z^*) I_j(r') dr' \quad (43)$$

where $j = 1, 2, 3, 4, 5, 6$. Then Eq. (28) can be rewritten as

$$E_{tan}^{\theta_b}(r) = \frac{-i\omega\mu_0}{(2\pi)^2} [A_o V_1(r) + B_o V_2(r) + C_o V_3(r) + A_e V_4(r) + B_e V_5(r) + C_e V_6(r)] \quad (44)$$

Next, we multiply a function $I_i(r)$ on both sides of the above equation and make an integration to r from $-h$ to h . By repeating this procedure for all I_1 - I_6 and using the boundary condition (33), Eq. (44) can be reformulated in terms of matrix multiplication. We write

$$V_0 \cdot \tilde{I} = \frac{i\omega\mu_0}{(2\pi)^2} (\tilde{T} \cdot \tilde{D}) \quad (45)$$

where

$$\tilde{I} = [I_1(0) \ I_2(0) \ I_3(0) \ I_4(0) \ I_5(0) \ I_6(0)]' \quad (46)$$

$$\tilde{D} = [A_o \ B_o \ C_o \ A_e \ B_e \ C_e]' \quad (47)$$

Here, the superscript ' $'$ in above vectors represents matrix transpose, and \tilde{T} is a 6×6 matrix with each of its element expressed as

$$T_{ij} = \int_{-h}^h \int_{-h}^h G(\rho^*, \varphi^*, z^*) I_i(r) I_j(r') dr' dr \quad (48)$$

It should be pointed out that the above formula contains the kernel function of the antenna as defined in (29), whose integrand is a highly oscillating function and thereby not suitable for direct integration. Hence, in the next section, we will further process the kernel function $G(\rho^*, \varphi^*, z^*)$ with some analytical techniques.

C. EVALUATION OF THE KERNEL FUNCTION

According to Eq. (8), the denominator of the integrand of $G(\rho^*, \varphi^*, z^*)$ can be written in the following form

$$B(k_z, \lambda) = k_0^2 \varepsilon_3 \left[k_z^2(\lambda) - k_1^2(\lambda) \right] \left[k_z^2(\lambda) - k_2^2(\lambda) \right] \quad (49)$$

where $\pm k_1$ and $\pm k_2$ are the zeros of $B(k_z, \lambda)$. We have

$$k_1^2(\lambda) = \frac{-b(\lambda) + \sqrt{b^2(\lambda) - 4c(\lambda)}}{2} \quad (50)$$

$$k_2^2(\lambda) = \frac{-b(\lambda) - \sqrt{b^2(\lambda) - 4c(\lambda)}}{2} \quad (51)$$

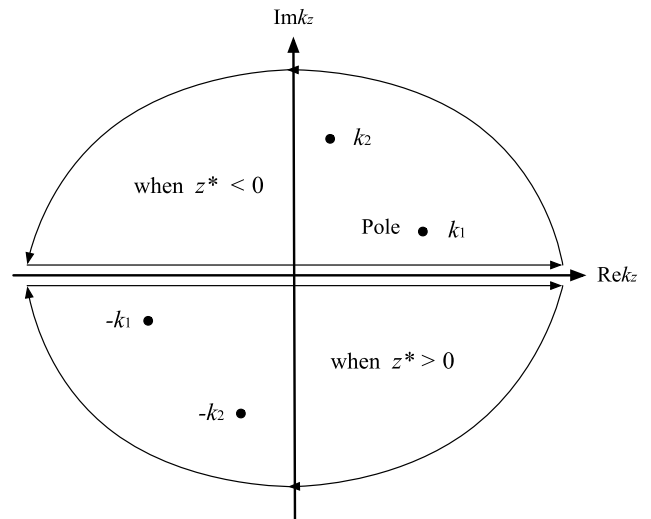


FIGURE 2. Selection of the integration path in the k_z plane.

where

$$b(\lambda) = \lambda^2 \left(1 + \frac{\varepsilon_1}{\varepsilon_3} \right) - 2k_0^2 \varepsilon_1 \quad (52)$$

$$c(\lambda) = \lambda^4 \left(\frac{\varepsilon_1}{\varepsilon_3} \right) + \lambda^2 k_0^2 \left(\frac{\varepsilon_2^2 - \varepsilon_1^2}{\varepsilon_3} - \varepsilon_1 \right) + k_0^4 (\varepsilon_1^2 - \varepsilon_2^2) \quad (53)$$

If we define the two zeros in the upper plane of k_z as k_1 and k_2 , then $-k_1$ and $-k_2$ must have negative imaginary parts. It is seen that $\pm k_1, \pm k_2$ are also the poles of the integrand of $G(\rho^*, \varphi^*, z^*)$. By applying the residue theorem, the integral with respect to k_z can be further expressed with the sum of residues at the poles. To ensure the wave always decays with the propagation distance, $\exp(-ik_z z^*)$ must be an attenuating factor. Thus, we let the integration path close from the upper plane of k_z (containing the poles of k_1 and k_2) when $z^* < 0$, and let the path close from the lower plane (containing $-k_1$ and $-k_2$) if $z^* > 0$. A schematic diagram illustrating the selection of the integration path is shown in Fig. 2. Considering all of the above, Eq. (29) could be rewritten as

$$G(\rho^*, \varphi^*, z^*) = \pm \frac{\pi i}{k_0^2 \varepsilon_3} \left[\int_0^\infty (Res_1 + Res_2) J_0(\lambda \rho^*) \lambda d\lambda + \int_0^\infty (Res_3 + Res_4) J_1(\lambda \rho^*) \lambda d\lambda \right] \quad (54)$$

where “+” corresponds to $z^* < 0$ and “-” corresponds to $z^* > 0$. Also, the four residues at k_1 and k_2 are given by

$$Res_1 = \exp(ik_1|z^*|) \times \frac{\cos^2 \theta_b S_1(k_1, \lambda) + \sin^2 \theta_b S_2(k_1, \lambda, \varphi^*)}{k_1(k_1^2 - k_2^2)} \quad (55)$$

$$Res_2 = \exp(ik_2|z^*|) \times \frac{\cos^2 \theta_b S_1(k_2, \lambda) + \sin^2 \theta_b S_2(k_2, \lambda, \varphi^*)}{k_2(k_2^2 - k_1^2)} \quad (56)$$

TABLE 1. Amplitude coefficients for the O-wave and E-wave at different geomagnetic inclination angles.

θ_b	0°	15°	30°	45°	60°	75°	89°
Re A_o	1.35×10^6	-1.23×10^3	-1.24×10^2	-4.70×10^0	2.33×10^0	2.10×10^{-1}	5.42×10^{-7}
Im A_o	-9.62×10^4	-1.36×10^2	-1.52×10^0	4.98×10^{-2}	-1.09×10^{-3}	1.42×10^{-5}	1.12×10^{-7}
Re B_o	3.46×10^{12}	-6.93×10^9	1.11×10^9	7.48×10^8	-1.02×10^6	-2.98×10^3	2.82×10^{-2}
Im B_o	-2.46×10^{12}	1.60×10^8	-3.79×10^7	-7.69×10^7	-4.15×10^2	1.68×10^{-1}	7.10×10^{-4}
Re C_o	-1.32×10^{13}	2.71×10^{10}	-4.50×10^9	-3.00×10^9	3.48×10^6	4.41×10^3	-1.13×10^{-1}
Im C_o	9.80×10^{12}	-7.02×10^8	1.51×10^8	3.08×10^8	1.95×10^3	-1.18×10^0	-2.90×10^{-3}
Re A_e	-8.92×10^2	9.40×10^{-1}	1.63×10^{-1}	4.07×10^{-2}	2.34×10^{-2}	-1.14×10^{-4}	3.88×10^{-11}
Im A_e	6.36×10^1	1.04×10^{-1}	2.01×10^{-3}	-3.29×10^{-4}	-1.09×10^{-5}	-7.74×10^{-9}	8.01×10^{-12}
Re B_e	1.37×10^3	-1.42×10^0	-2.33×10^{-1}	-5.27×10^{-2}	-2.48×10^{-2}	7.43×10^{-5}	4.23×10^{-11}
Im B_e	-9.78×10^1	-1.57×10^{-1}	-2.88×10^{-3}	4.31×10^{-4}	1.16×10^{-5}	5.04×10^{-9}	8.73×10^{-12}
Re C_e	-2.03×10^3	2.04×10^0	2.99×10^{-1}	5.00×10^{-2}	5.62×10^{-3}	1.55×10^{-4}	-3.74×10^{-11}
Im C_e	1.45×10^2	2.26×10^{-1}	3.68×10^{-3}	-4.18×10^{-4}	-2.62×10^{-6}	1.05×10^{-8}	-7.70×10^{-12}

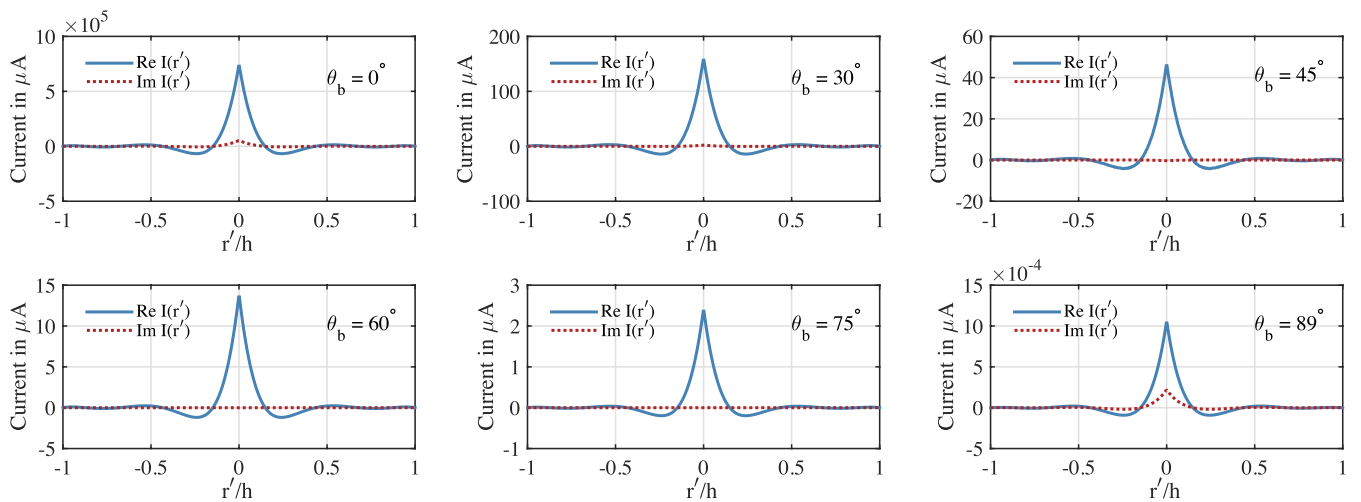


FIGURE 3. Current distributions on the antenna at several different geomagnetic inclination angles.

$$Res_3 = \exp(ik_1|z^*|) \times \frac{\sin^2 \theta_b S_3(k_1, \lambda, \varphi^*) + \sin \theta_b \cos \theta_b S_4(k_1, \lambda, \varphi^*)}{k_1(k_1^2 - k_2^2)} \quad (57)$$

$$Res_4 = \exp(ik_2|z^*|) \times \frac{\sin^2 \theta_b S_3(k_2, \lambda, \varphi^*) + \sin \theta_b \cos \theta_b S_4(k_2, \lambda, \varphi^*)}{k_2(k_2^2 - k_1^2)} \quad (58)$$

Now $G(\rho^*, \varphi^*, z^*)$ has been reduced to a single infinite integral containing the Bessel functions J_0 and J_1 . By applying fast Hankel transforms to J_0 and J_1 as is addressed in [26]–[28], the integral of (54) can be numerically evaluated with guaranteed accuracy. Once the kernel function is computed, the components of \tilde{T} are readily obtained through numerical methods, and the current distribution on

the antenna can be completely determined by solving the six amplitude coefficients. Furthermore, the input impedance of the antenna Z_{in} is also obtained readily. We write

$$Z_{in} = \frac{V_0}{I(0)} \quad (59)$$

So far, we have derived the method for calculating the current distribution and input impedance of an arbitrarily oriented linear antenna in an anisotropic plasma. Next, the corresponding computations will be carried out.

III. COMPUTATIONS AND DISCUSSIONS

With the above methods, computations are carried out when the antenna is placed at different angles to the geomagnetic field. The results for the six amplitude coefficients are listed in Table 1, and those for the current distribution are shown in Fig. 3. The parameters used in the computations are

TABLE 2. Wave numbers, wave lengths, and input impedances at several different geomagnetic inclination angles.

θ_b	β_o	α_o	β_e	α_e	$\text{Re}(n_e)$	λ_e	$ Z_{in} $ when $2h/\lambda_e =$			
							1/4	1/3	1/2	3/4
0°	1.21×10^{-6}	0.0209	0.0211	1.24×10^{-6}	80.64	297.4 m	1.02 Ω	1.73 Ω	2.50 k Ω	2.51 Ω
15°	1.27×10^{-6}	0.0213	0.0215	1.31×10^{-6}	82.06	292.3 m	910.01 Ω	1.11 k Ω	2.13 M Ω	2.19 k Ω
30°	1.49×10^{-6}	0.0225	0.0227	1.54×10^{-6}	86.72	276.6 m	3.85 k Ω	5.59 k Ω	8.02 M Ω	9.90 k Ω
45°	2.02×10^{-6}	0.0248	0.0252	2.10×10^{-6}	96.08	249.6 m	23.44 k Ω	14.75 k Ω	29.06 M Ω	30.11 k Ω
60°	3.36×10^{-6}	0.0295	0.0300	3.55×10^{-6}	114.57	209.3 m	67.81 k Ω	49.85 k Ω	88.74 M Ω	89.84 k Ω
75°	8.81×10^{-6}	0.0406	0.0421	9.80×10^{-6}	160.66	149.3 m	158.26 k Ω	230.58 k Ω	409.86 M Ω	421.74 k Ω
89°	2.81×10^{-4}	0.1288	0.2316	1.63×10^{-3}	883.90	27.1 m	48.90 M Ω	75.77 M Ω	137.72 G Ω	195.84 M Ω

taken as follows: the operating frequency is $f = 12.5$ kHz, the magnitude of the geomagnetic field is $B_0 = 0.5 \times 10^{-4}$ T, and the electron density and collision frequency of the ionosphere are taken as $N = 1.4 \times 10^{12} \text{ m}^{-3}$, $\nu = 10^3 \text{ s}^{-1}$, respectively. Thereby we have $\omega_0 = 6.6 \times 10^7 \text{ arc/s}$, $\omega_H = 8.6 \times 10^6 \text{ arc/s}$, and the condition $\omega_0 > \omega_H > \omega$ is satisfied. Besides, the feeding voltage is $V_0 = 1$ V, and the length and radius of the linear antenna are taken as $2h = 100$ m, $a = 0.01$ m, respectively. It is addressed in [20] that the E-wave is a propagable wave only when the propagation direction is within the critical angle. The critical angle θ_c is determined by the following equation

$$\theta_c = \tan^{-1} \sqrt{\frac{\epsilon_3}{\epsilon_1}} \tag{60}$$

Since $\theta_c \approx 89^\circ$ in the VLF range, the range of θ_b used in our computations is between $0^\circ \sim 89^\circ$.

From Table 1 it is found that the magnitude of the coefficients for the O-wave is obviously greater than that for the E-wave. Despite the six amplitude coefficients vary significantly with θ_b , the current distributions in Fig. 3 are all close to triangular distributions and are very similar to each other no matter how the geomagnetic inclination angle changes. This is because a 100-m space-borne linear antenna is technically not an electrically short antenna due to the high refractive index of the ionosphere at the VLF range, thus its current distribution is slightly deviated from a triangular distribution [17]. It is also noticed that when θ_b is larger, all the coefficients will become smaller and the current on the antenna will decrease rapidly. We may infer that the current distribution on a VLF space-borne linear antenna is not sensitive to the orientation of the antenna, but the amplitude of the current will diminish as the geomagnetic inclination angle increases. As is observed from Fig. 3, the current always reaches its maximum at the feeding point, and will gradually reduce to zero at the two terminals. This indicates that the effective radiation units mainly concentrate on the middle part of the antenna, and how to increase the total current moment on the antenna with limited power will be the key to improve the efficiency of a space-borne linear antenna.

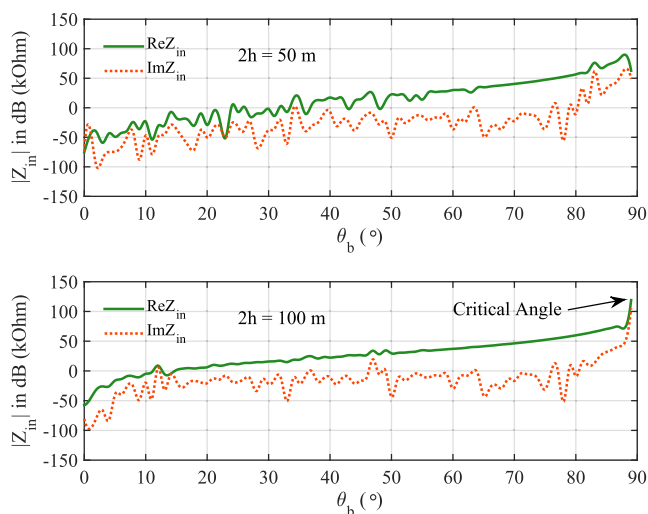


FIGURE 4. Input impedance of the antenna varying with the geomagnetic inclination angle.

Fig. 4 shows the results of the input impedance of the antenna varying with the geomagnetic inclination angle. All parameters are same with those used in Fig. 3 except the antenna length is taken as $2h = 50$ and 100 m, respectively. It is found that because of the complex anisotropic properties of the ionospheric plasma in the VLF range, there will be dramatic variations on the input impedance of the antenna as θ_b changes, and this phenomenon is more evident if the antenna is shorter. Despite those fluctuations, the overall trend for the input impedance is increasing with θ_b , which indicates that the efficiency of a VLF space-borne linear antenna will be decreased when the geomagnetic inclination angle becomes larger. This conclusion is in good agreement with the ones drawn in [12] and [17] that the power delivery is optimal for an antenna parallel to the static magnetic field. And a possible reason for that is the wave numbers for the O-wave and E-wave in an anisotropic ionosphere are also varying with the propagation direction. Table 2 lists the values of β_o , α_o , β_e , and α_e at several different θ_b , in which one may see that the attenuation rates for both the O-wave and E-wave will increase with the inclination angle of the

antenna. This could explain why the input impedance shown in Fig. 4 will keep increasing as θ_b approaches θ_c . Therefore, in order to realize maximum antenna efficiency in practical applications, the optimal orientation for a VLF space-borne linear antenna should be as parallel as possible to the direction of the geomagnetic field.

Table 2 also provides the corresponding refractive indices (n_e) and wavelengths (λ_e) for the E-wave at different θ_b , as well as the input impedances at several typical antenna lengths. It follows that because of the high refractive index of the ionosphere in the VLF range, the wavelength of the E-wave is greatly shortened in the ionosphere. Also, both the refractive index and wavelength in an anisotropic plasma are dependent on the propagation direction. Since the refractive index increases with θ_b , the wavelength for the propagable mode in the ionosphere will become shorter when the inclination angle is larger. As is different with that in an isotropic medium, the half-wavelength antenna does not have a smallest input impedance in this case. Nevertheless, the input impedances of a 1/4-wavelength or 1/3-wavelength antenna seem to be relatively small. Finally, as similar as those shown in Fig. 4, the input impedances at all antenna lengths will increase with the geomagnetic inclination angle.

IV. CONCLUSIONS

In this paper, the problem of a VLF linear antenna of arbitrary orientation in a homogeneous anisotropic cold plasma is treated both analytically and numerically. The kernel function in this case includes the effect of the geomagnetic inclination angle and thus has a more complicated form. The obtained results are particularly applicable for small drive voltages so that those nonlinear sheath effects are allowed for omission. Computations show that the amplitude coefficients for the O-wave are much greater than those for the E-wave, and the current distribution on the antenna is not sensitive to the orientation of the antenna. It is also found that the overall trend for the input impedance of the antenna will increase with the geomagnetic inclination angle, and because of that, the total current moment on the antenna is decreased when the inclination angle becomes larger. In order to maximize the antenna efficiency, the optimal posture for a VLF space-borne linear antenna should be as parallel as possible to the geomagnetic field since the antenna has a smallest input impedance when θ_b tends to zero. Moreover, we found that the half-wavelength antenna is not highly efficient in an anisotropic plasma, while the 1/4-wavelength or 1/3-wavelength antennas have a more promising input impedance. With the fast development of space technology, space-borne transmitters will play a more and more important role in contemporary VLF transmitting systems. Hence, the proposed method might be helpful to practical space-borne applications for cases where the antenna orientation is variable.

REFERENCES

- [1] R. A. Helliwell, *Whistlers and Related Ionospheric Phenomena*, 2nd ed. Mineola, NY, USA: Dover, 2006, pp. 23–24.
- [2] K. Rawer, D. Bilitza, and S. Ramakrishnan, “Goals and status of the international reference ionosphere,” *Rev. Geophys.*, vol. 16, pp. 177–181, May 1978.
- [3] J. A. Carroll, “The small expendable deployment system (SEDS),” in *Proc. 2nd Int. Conf. Space Tethers Sci. Space Station Era*, Venice, Italy, Oct. 1987, pp. 43–50.
- [4] N. A. Armand, I. P. Semenov, B. E. Chertok, V. V. Migulin, and V. V. Akindinov, “Experimental investigation of the VLF radiation of a loop antenna installed on the Mir-progress-28-Soyuz TM-2 orbital complex in the earth’s ionosphere,” (in Russian), *Radiotekhnika Elektronika*, vol. 33, pp. 2225–2233, Nov. 1988.
- [5] R. Deloach, J. Diamond, T. Finley, and R. Rhew, “End-mass instrumentation for the first SEDS/Delta II mission,” in *Proc. 28th AIAA Aerosp. Sci. Meeting*, Reno, NV, USA, Jan. 1990, p. 537.
- [6] P. R. Bannister, J. K. Harrison, C. C. Rupp, R. W. P. King, M. L. Cosmo, E. C. Lorenzini, C. J. Dyer, and M. D. Grossi, “Orbiting transmitter and antenna for spaceborne communications at ELF/VLF to submerged submarines,” in *Proc. AGARD, ELF/VLF/LF Radio Propag. Syst. Aspects*, vol. 529, May 1993, pp. 1–14.
- [7] V. A. Koshelev and V. M. Melnikov, *Large Space Structures Formed by Centrifugal Forces*. Boca Raton, FL, USA: CRC Press, 1998.
- [8] TSS. *NASA Science Missions*. Accessed: Jan. 18, 2019. [Online]. Available: <http://science.nasa.gov/missions/tss/>
- [9] K. Balmain, “The impedance of a short dipole antenna in a magnetoplasma,” *IEEE Trans. Antennas Propag.*, vol. AP-12, no. 5, pp. 605–617, Sep. 1964.
- [10] T. N. C. Wang and T. F. Bell, “Radiation resistance of a short dipole immersed in a cold magnetoionic medium,” *Radio Sci.*, vol. 4, no. 2, pp. 167–177, Feb. 1969.
- [11] T. N. C. Wang and T. F. Bell, “On VLF radiation resistance of an electric dipole in a cold magnetoplasma,” *Radio Sci.*, vol. 5, no. 3, pp. 605–610, Mar. 1970.
- [12] T. N. C. Wang and T. F. Bell, “VLF/ELF radiation patterns of arbitrarily oriented electric and magnetic dipoles in a cold lossless multicomponent magnetoplasma,” *J. Geophys. Res.*, vol. 77, no. 7, pp. 1174–1189, Mar. 1972.
- [13] N. Vernet, R. Manning, and J. L. Steinberg, “The impedance of a dipole antenna in the ionosphere, 1, experimental study,” *Radio Sci.*, vol. 10, no. 5, pp. 517–527, May 1975.
- [14] P. Meyer and N. Vernet, “The impedance of a dipole antenna in the ionosphere, 2, comparison with theory,” *Radio Sci.*, vol. 10, no. 5, pp. 529–536, May 1975.
- [15] P. Nikitin and C. Swenson, “Impedance of a short dipole antenna in a cold plasma,” *IEEE Trans. Antennas Propag.*, vol. 49, no. 10, pp. 1377–1381, Oct. 2001.
- [16] T. F. Bell, U. S. Inan, and T. Chevalier, “Current distribution of a VLF electric dipole antenna in the plasmasphere,” *Radio Sci.*, vol. 41, no. 2, pp. 1–14, Apr. 2006.
- [17] T. W. Chevalier, U. S. Inan, and T. F. Bell, “Terminal impedance and antenna current distribution of a VLF electric dipole in the inner magnetosphere,” *IEEE Trans. Antennas Propag.*, vol. 56, no. 8, pp. 2454–2468, Aug. 2008.
- [18] Y. V. Chugunov, E. A. Shirokov, and I. A. Fomina, “On the theory of a short cylindrical antenna in anisotropic media,” *Radiophys. Quantum Electron.*, vol. 58, no. 5, pp. 318–326, Oct. 2015.
- [19] T. He, X. W. Zhang, W. Y. Pan, and K. Li, “Current distribution and input impedance of a VLF linear antenna in an anisotropic plasma,” *IEEE Trans. Antennas Propag.*, vol. 67, no. 3, pp. 1519–1526, Mar. 2019.
- [20] K. Li and W. Pan, “Radiation of an electric dipole in an anisotropic medium,” *Indian J. Radio Space Phys.*, vol. 26, pp. 340–345, Dec. 1997.
- [21] T. H. Oswald, W. Macher, H. O. Rucker, G. Fischer, U. Taubenschuss, J. L. Bougeret, A. Lecacheux, M. L. Kaiser, and K. Goetz, “Various methods of calibration of the STEREO/WAVES antennas,” *Adv. Space Res.*, vol. 43, pp. 355–364, Feb. 2009.
- [22] H. G. James, “A review of the major developments in our understanding of electric antennas in space plasmas,” *URSI Radio Sci. Bull.*, vol. 2011, no. 336, pp. 75–94, Mar. 2011.
- [23] W.-Y. Pan and K. Li, *Propagation of SLF/ELF Electromagnetic Waves*. Berlin, Germany: Springer-Verlag, 2014, ch. 7.
- [24] I. S. Gradshteyn and I. M. Ryzhik, *Table of Integrals, Series, and Products*, 7th ed. Amsterdam, The Netherlands: Elsevier, 2007.
- [25] R. W. P. King, G. S. Smith, M. Owens, and T. T. Wu, *Antennas in Matter: Fundamentals, Theory, and Applications*. Cambridge, MA, USA: MIT Press, 1981.

- [26] H. K. Johansen and K. Sørensen, "Fast Hankel transforms," *Geophys. Prospecting*, vol. 27, no. 4, pp. 876–901, Dec. 1979.
- [27] D. Guptasarma and B. Singh, "New digital linear filters for Hankel J_0 and J_1 transforms," *Geophys. Prospecting*, vol. 45, no. 5, pp. 745–762, Sep. 1997.
- [28] F. N. Kong, "Hankel transform filters for dipole antenna radiation in a conductive medium," *Geophys. Prospecting*, vol. 55, no. 1, pp. 83–89, Jan. 2007.



TONG HE (SM'18) was born in Hangzhou, Zhejiang, China, in 1990. He received the B.S. degree in electrical engineering and automation from the University of Electronic Science and Technology of China (UESTC), Chengdu, Sichuan, China, in 2013, and the M.S. degree in electrical engineering from the University of Michigan–Dearborn, Dearborn, MI, USA, in 2014. He is currently pursuing the Ph.D. degree in electromagnetic field and microwave technology with the College of Information Science and Electronic Engineering, Zhejiang University, Hangzhou, Zhejiang, China.

His current research interests include VLF wave propagation and antenna theory.



propagation and antenna theory.

HUI RAN ZENG (SM'19) was born in Chongqing, China, in 1995. She received the B.S. degree in electronic and information engineering from the East China University of Science and Technology, Shanghai, China, in 2017. She is currently pursuing the Ph.D. degree in electromagnetic field and microwave technology with the College of Information Science and Electronic Engineering, Zhejiang University, Hangzhou, Zhejiang, China. Her current research interests include radio wave



KAI LI was born in Xiao, Anhui, China, in 1968. He received the B.S. degree in physics from Fuyang Normal University, Fuyang, Anhui, China, in 1990, the M.S. degree in radio physics from Xidian University, Xi'an, Shaanxi, China, in 1994, and the Ph.D. degree in astrophysics from the Shaanxi Astronomical Observatory, Chinese Academy of Sciences, Xi'an, in 1998.

From 1990 to 2000, he was a Faculty of the China Research Institute of Radiowave Propagation (CRIRP), Xinxiang, Henan, China. From 2001 to 2002, he was a Postdoctoral Fellow with the Information and Communications University (ICU), Daejeon, South Korea. From 2003 to 2005, he was a Research Fellow with the School of Electrical and Electric Engineering, Nanyang Technological University (NTU), Singapore. Since 2005, he has been a Professor with the College of Information Science and Electronic Engineering, Zhejiang University, Hangzhou, China. His current research interests include classic electromagnetic theory and radio wave propagation.

Dr. Li is a Senior Member of the Chinese Institute of Electronics (CIE) and a member of the Chinese Institute of Space Science (CISS).

• • •